Powder Technology 355 (2019) 675–687

Contents lists available at ScienceDirect

Powder Technology

journal homepage: www.elsevier.com/locate/powtec

Comprehensive study of co-processed excipients F- Melts®: Flow, viscoelastic and compacts properties

Petra Svačinová [a], Barbora Vraníková [a], Martin Dominik [b], Jan Elbl [b,*], Sylvie Pavloková [b], Roman Kubalák [b], Pavlína Kopecká [b], Aleš Franc [b]

[a] Department of Pharmaceutical Technology, Faculty of Pharmacy in Hradec Kralove, Charles University, Akademika Heyrovskeho 1203, Hradec Kralove 500 05, Czech Republic
[b] Department of Pharmaceutics, Faculty of Pharmacy, Veterinary and Pharmaceutical University Brno, Palackého tr. 1946/1, Brno 612 42, Czech Republic

ARTICLE INFO

Article history:
Received 21 December 2018
Received in revised form 30 May 2019
Accepted 12 July 2019
Available online 15 July 2019

Keywords:
Co-processed excipients
Direct compression
Orally dispersible tablets
F-melt
Neusilin
Fujicalin

ABSTRACT

This article aims to compare three commercially available co-processed excipients (CPEs), namely the F-Melts® type C, M and F1. All three CPEs were subjected to the evaluation of their physical properties and afterwards compacts were prepared using three compression pressures. The viscoelastic properties and ejection force were assayed during the compression and the compacts were evaluated in compliance with the European Pharmacopoeia and subjected to other relevant testing (AFM imaging, wettability etc.). Based on the obtained results it could be stated that the C and M have very similar properties according to their similar composition. In general, it is difficult to select the best CPE as they possess different properties fitting the versatile needs of manufacturers. However, the obtained results revealed that the M and F1 are more suitable for the incorporation of moisture-sensitive ingredients than the C.

1. Introduction

Orally dispersible tablets (ODTs) rapidly disintegrate after their administration to the oral cavity forming an easily swallowable dispersion that is advantageous for patients with swallowing difficulties (children, seniors, psychiatric and dysphagia patients). As ODTs are liquefied in mouth, they combine the benefits of liquid and conventional solid dosage forms, such as good stability, easy dosing, and swallowing connected with high bioavailability of the administered drug. One of the widely used methods for the production of ODTs is the direct compression (DC) [1,2].

The principle lies simply in weighing, blending and compressing the appropriate components. Thus gaining the advantages of a limited number of manufacturing steps, reduced time of manufacturing and lower energy demands. This results in cost reduction, lower variability of the production, an improved stability of the active substance (API), shorter disintegration and dissolution of manufactured tablets, easier validation of the production and a lower risk of microbial contamination [3]. On the other hand, by omitting the granulation process, manufacturing of tablets with a high content of active ingredients (API) is limited, as particles of API often segregate during blending, which may negatively influence the content uniformity. Moreover, due to a powder blend usually having worse flow properties, the weight variability may also increase [4]. Furthermore, the higher surface area of the powder blend requires the addition of a larger amount of the lubricant. The tablets may also have lower mechanical resistance, which can be observed during the stress testing [5]. To address these limitations and disadvantages, producers decided to refine direct compression excipients. Firstly, mono-excipients with improved flow properties and compressibility were introduced. Secondly, co-processed excipients (CPEs) were put in practice. CPEs are blends containing mostly fillers, binders, and disintegrants and sometimes also surfactants or lubricants. These blends are processed by various technologies, such as melt granulation, dry granulation, wet granulation, fluid bed granulation and co-crystallisation, but mainly spray drying (SpD) [6]. The SpD leads to the formation of highly porous particles with good flowability and tabletability, while ensuring short-time disintegration in the physiological fluids, particularly in saliva. Usually the spherical shape of the newly formed particles improves the flow properties and provides a better rearrangement of the particles in the die during tableting, resulting in better compaction characteristics [7]. However, although the composition of these CPEs may be virtually similar, the small changes in the components' characteristics can make them behave differently after compression [8].

The novel excipients F-Melts® (C, M and F1) belonging to the CPEs prepared by the SpD technique are dedicated especially for the manufacturing of ODTs by DC. The type C is suitable for pharmaceutical

* Corresponding author at: Department of Pharmaceutics, Faculty of Pharmacy, Veterinary and Pharmaceutical University Brno, Palackého tr. 1946/1, Brno 612 42, Czech Republic.
E-mail address: elblj@vfu.cz (J. Elbl).

https://doi.org/10.1016/j.powtec.2019.07.048
0032-5910/

and nutraceutical formulations; the M for pharmaceutical preparations only while the F1 for nutraceutical/dietary supplements. Their patented composition is based on carbohydrates, an inorganic excipient and a disintegrating agent. Mannitol and xylitol in the form of complex particles are present as carbohydrates in types C and M, while the inorganic excipient and the disintegrating agent are dispersed in these complex particles [9]. The inorganic excipients are represented by magnesium aluminometasilicate (Neusilin®) in the case of type C, and calcium hydrogen phosphate anhydrous (Fujicalin®) in the case of type M. Crospovidone in the combination with microcrystalline cellulose (MCC) is used as a disintegrant in both mentioned types of F-Melt® [10]. The type F1 differs in composition as it contains waxy rice starch, Fujicalin® and microcrystalline cellulose. The type C conforms to USP-NF, EP and JP and the type M conforms to USP-NF and JP [11].

The novel excipients present in the composition of F-Melts® Neusilin® and Fujicalin® are mostly used in DC, wet granulation or preparation of liquisolid systems. They are widely used for the improvement of the quality of tablets, powders, granules and capsules. Neusilin® occurs as a fine powder or in the form of granules and it increases the hardness synergy with other fillers and binders [12]. Its large specific surface area allows to adsorb a high quantity of liquids (e.g. drug in liquid state, humidity) and therefore to stabilize the moisture sensitive as well as lipophilic substances [13]. Fujicalin® is in the form of porous, free flowing spheres with an extensive specific surface area [14]. The particles are highly stable and provide higher tensile strength to tablets when compacted [15]. According to the manufacturer, a combination of these patented substances and other excipients in the form of co-processed excipients offers an easy DC formulation of ODTs with the optimal tablet hardness of above 50 N, fast oral disintegration time of <30 s and >50% of drug loading [11]. Furthermore, the tablets should provide a pleasant mouthfeel and hence increase the patient's compliance [16].

At the moment, pharmaceutical companies are facing a mounting pressure on producing more dosage forms in shorter time both in the development and in manufacturing of final preparations. The already published information may significantly decrease the time spent on rigorous formulation testing [17,18]. Although there are data available on CPEs physico-chemical properties, they are distributed among various sources such as reviews, experimental works and producers´ information. This state does not provide a whole proof compatibility of the mentioned data [19–23].

The aim of this work was the comparison of these three commercially available types of the F-Melt® excipients on the basis of physico-chemical characteristics obtained by identical methods and apparatus. Therefore, these individual CPEs were complexly evaluated for their flow properties including the angle of slide, sieve analysis, specific surface area, moisture content, hygroscopicity, solubility, pH leaching, electrostatic charge, and compressibility without lubricant. Mass uniformity, pycnometric density, height, tensile strength, friability, disintegration, wetting rate, and water absorption ratio were evaluated for the compacts. The SEM was performed for both CPEs and compacts, while the AFM imaging was used to characterize the compacts' surface. Some of the results have never been published. Since the specific properties of these individual excipients can be selectively overlapped by the addition of another substance according to their nature, no model drugs have been added. The obtained data may help producers to choose suitable excipients for tablet formulation and to find out dependencies between the composition and tablets' behaviour in the oral cavity.

2. Materials and methods

2.1. Materials

The F-Melt® C, F-Melt® M and F-Melt® F1 were all manufactured by Fuji Chemical Industries Co., Ltd.

2.2. Methods

2.2.1. Flow properties

The flow rate of the CPEs through a 15 mm diameter orifice was measured on a flowability tester according to Ph. Eur. The measurements were performed in triplicate and the results are expressed as mean values ± standard deviation.

The angle of repose (α) was determined according to Ph. Eur. by measuring the height and the base diameter of the cone formed by 100 g of powder. The measurements were performed in triplicate and the results are expressed as mean values ± standard deviation.

The angle of slide was tested with the powder sample (10 g) placed on one end of a metal plate with a polished surface. This end was gradually raised until the sample was about to slide. The angle formed between the plate and the horizontal surface at the slide moment was measured [24]. The measurements were performed in triplicate and the results are expressed as mean values ± standard deviation.

The bulk and tapped volumes were evaluated in a tapped density tester (SVM 102, Erweka GmbH, Germany) and subsequently used to calculate the bulk and tapped densities, Hausner ratio (HR), Carrs' compressibility index (CI) according to Ph. Eur.

2.2.2. Pycnometric density and porosity of powders

The true density (ρ) of the CPE was determined by the gas displacement technique using the helium pycnometer (Pycnomatic ATC, Ing. Prager Elektronik Handels GmbH, Austria), according to Ph. Eur. All density measurements were performed in triplicate and the results are expressed as mean values ± standard deviation. The porosity of CPE was calculated according to the equation:

$$porosity = \left(1 - \frac{\rho_{pycnometric}}{\rho_{bulk}}\right) \cdot 100 \quad (1)$$

2.2.3. Sieve analysis

The particle size distribution was evaluated by a sieve analysis using a set of stainless steel sieves with apertures ranging from 0.025 to 0.800 mm placed on a vibratory sieve shaker (AS 200 basic, Retsch GmbH &Co. KG, Ingelheim, Germany). The percentage weight of the mass retained on each of the sieves was determined.

2.2.4. Mean particle size

The particle size was determined by laser diffraction of dry samples (HELOS KR, SYMPATEC GmbH, Germany). D_{10}, D_{50}, D_{90} are the diameters of a sample at the 10th, 50th and 90th percentiles of the cumulative percent undersize plot. The measurements were performed in duplicate and the results are expressed as mean values.

2.2.5. Specific surface area

The specific surface area was determined by nitrogen adsorption (MSP, Geotest Brno, Czech Republic). The samples were degassed at 200 °C in vacuum for 24 h before the measurement. The specific surface area was obtained from the Brunauer-Emmett-Teller (BET) model [25] using 0.162 nm^2 as the area occupied by one nitrogen molecule. Powdered Titan Oxide (SSA = 13.76 m^2/g) was used as a standard. The measurements were performed in triplicate and the results are expressed as mean values.

2.2.6. Moisture content

The percentage of moisture content in the co-processed excipients was assayed in a halogen moisture analyser (Mettler Toledo, HX204, Switzerland) under the following conditions: standard drying program, drying temperature of 105 °C, switch-off criterion 1 mg of mass loss in 50 s. The measurements were performed in duplicate and the results are expressed as mean values ± standard deviation.

2.2.7. Hygroscopicity

Hygroscopicity was measured in a constant climate chamber (Binder, KBF 240, Germany) under the following conditions: the temperature of 40 °C, humidity of 75% RV and duration for 30 days. Three grams of the samples were examined in 0.25, 0.5, 1, 3, 5, 8, 24, 72, 120, 168 and 720 h in a halogen moisture analyser (Mettler Toledo, HX204, Switzerland). The measurements were performed in duplicate and the results are expressed as mean values ± standard deviation.

2.2.8. Solubility

The percentage of the soluble fraction of CPE was determined. The first phase was to evaluate the insoluble fraction at the physiological amount of saliva (15 ml) in mouth to simulate the oral cavity. One gram of the sample was dried in a hot air dryer (Horo, Type 38A, Germany) at 60 °C for 4 h. It was weighed after drying and dissolved in 15 ml of artificial saliva by stirring at 600 rpm in a mechanical stirrer (HEIDOLPH RZR 2021, Sigma Aldrich, USA) for 3 min. The time limit of 3 min was chosen according to the pharmacopoeial disintegration test for ODTs. The solution was filtered through a filter paper pre-dried in a hot air dryer at 60 °C for 4 h. The filter paper with undissolved solids was dried again at 60 °C for 4 h. The percentage of the undissolved fraction was calculated from the weight difference of the filter paper with and without the sample. The measurements were performed in duplicate and the results are expressed as mean values ± standard deviation.

The second phase was to determine the total soluble fraction. One gram of the sample was dried in a hot-air oven (60 °C, 4 h) and dissolved in 900 ml of artificial saliva by mechanical stirring at 600 rpm for 24 h. The artificial saliva was prepared according to the formula proposed by Hobbs et al. [26]. The following procedure was identical to the first evaluation method. The measurements were performed in duplicate and the results are expressed as mean values ± standard deviation.

2.2.9. pH leaching

The pH leaching was determined as the pH value of a 2% solution. The water for measurement was degassed by boiling for 1 min. The pH of the CPE solution was measured using a surface pH microelectrode connected to a pH meter (pH 210, Hanna Instruments, Mauritius).

2.2.10. Charge density

To evaluate the charge density, 25 g of the excipient were blended by a blender (Turbula T2C, Swiss) at 40 rpm in a glass container of 2 l volume. After 0, 5, 10 and 20 min of blending, the excipient was transferred to Faraday pail (JCI 150, Chilworth technology ltd.) connected to a calibrated charge measurement unit (JCI 178, Chilworth technology ltd.). The exact transferred mass of the excipient was weighted afterwards. The charge density was obtained by dividing the net charge by the mass of the excipient. The measurements were performed in duplicate and the results are expressed as mean values ± standard deviation.

2.2.11. Scanning electron microscopy (SEM)

The surface morphology of the CPE was examined by SEM. The samples were attached to aluminium stubs with a double-sided adhesive carbon tape, gold coated with a sputter coater (JEOL NeoCoater MP-19020NCTR, Japan) and examined using a scanning electron microscope (JEOL JCM-6000, Japan). The signals of the samples were produced by back-scattered electrons (BSE), at 15 kV voltage and different magnifications.

The compact surface morphology was characterized by means of scanning electron microscopy (SEM; MIRA3, Tescan Orsay Holding, Czech Republic). The samples were fixed onto a SEM specimen stub using a carbon conductive double-sided adhesive tape (Agar Scientific, United Kingdom) and then coated by a metal sputtering of Au under an argon atmosphere (Q150R ES Rotary-Pumped Sputter Coater/Carbon Coater, Quorum Technologies, United Kingdom). The signals of the samples were produced by secondary electrons (SE), using 3 or 5 kV voltage depending on the sample.

2.2.12. Differential scanning calorimetry

The differential scanning calorimetry (DSC) experiments were performed using the DSC 7 instrument (Perkin Elmer Instruments, USA). The heating rate and heat flow were calibrated at 10 °C/min using the indium and zinc standard. The heat flow rate was set at 10 °C/min and inert nitrogen atmosphere (3.5 Bar) was employed. Approximately 5 mg of every sample were weighed in vented aluminium pan with crimp-on lid. All samples were analysed over the temperature range 50–250 °C.

2.2.13. Compact preparation

Compacts with the cylindrical shape (diameter of 7 mm, mass of 200 mg) were compressed using the material testing machine (Zwick/Roell T1-FRO 50, Zwick GmbH, Germany) with the compaction punches and die (Adamus HT, Machine Factor Group, Poland). The compression pressures used were 78, 130 and 182 MPa at the compression rate of 0.5 mm/s. 55 compacts were compacted at each compression pressure from each material without the addition of any lubricants or glidants. The compacts were stored in a polyethylene bags for at least 24 h before testing.

2.2.14. Energy evaluation of compression process

The force-displacement record was employed to evaluate the energetic parameters. During the compression, the computer program testXpert V. 9.01 recorded the energy consumed for friction E_1 (J), plastic deformation E_2 (J) and the elastic energy released during decompression E_3 (J) [27]. The above-mentioned energies were used to calculate the plasticity (PL; %) according to the equation [28]:

$$PL = 100 * E_2/(E_2 + E_3) \quad (2)$$

The results of the measurement of 55 compacts are expressed as mean values ± standard deviation. For statistical evaluation, the *t*-test on the significance level $p = 0.05$ was used.

2.2.15. Ejection force

The ejection force was determined using the material testing machine (Zwick/Roell T1-FRO 50, Zwick GmbH, Germany). After the compression, the lower punch was removed and the ejection test was commenced. The ejection rate was 10 mm/min. The computer program testXpert V. 9.01 recorded the maximal ejection force. The results of 10 measurements are expressed as mean values ± standard deviation.

2.2.16. Uniformity of mass

Twenty randomly selected compacts from each sample were weighed individually on an analytical balance (HR-120, A&D Company, Japan). The results are expressed as mean values ± standard deviation.

2.2.17. AFM imaging

The surface roughness was visualised using the atomic force microscope (AFM) Nanosurf easyScan 2 FlexAFM (Nanosurf, Switzerland). The scans were performed in Tapping Mode using the Tap 190Al-G cantilevers (BudgetSensors, Bulgaria) with the spring constant from 28 to 75 N/m. Fifteen randomly selected areas of 10 × 10 μm were measured on the surface of the compacts compressed by pressure of 182 MPa. The resolution was 512 × 512 points. The surface roughness was expressed as the Root Mean Square Sq (nm). The results of 15 measurements are expressed as mean values ± standard deviation.

2.2.18. Pycnometric density and porosity of compacts

The gas displacement technique with a helium pycnometer (AccuPyc II 1340, Micromeritics, USA) was used to evaluate the pycnometric density of the compacts. The precisely weighed sample was introduced to the complete dry test cell. The test cell containing the sample was sealed in the pycnometer and the analysis started. The

measurements were performed five times and the results are expressed as mean values ± standard deviation.

The porosity of the compacts was calculated using the mean values of pycnometric density (ρ_{pyc}), compact mass (m) and compact volume (V) according to the Eq. (3) [29].

$$porosity\ of\ compacts = 1-\left[m/\left(\rho_{pyc}\cdot V\right)\right] \quad (3)$$

2.2.19. Compact height and tensile strength

The compact height, diameter and crushing force were measured in 10 compacts using a hardness tester (8 M, Dr. Schleuniger Pharmatron AG, Switzerland). The tensile strength of the compacts was calculated using the equation [30]:

$$TS = (2 \cdot F)/(\pi \cdot d \cdot h) \quad (4)$$

where *TS* (MPa) is the tensile strength, *F* (N) is the crushing force, *d* (mm) is the diameter of the compact and *h* (mm) is the height of the compact. The results of 10 measurements are expressed as mean values ± standard deviation.

2.2.20. Consolidation behaviour of powders

The calculation of consolidation behaviour of powders was based on the compact's volume (Eq. (5)), which was related to the bulk volume of the same weight of powder (200 mg). Eq. (6) was used for the calculation of the percentage loss in volume (consolidation).

$$V = \pi \cdot r^2 \cdot h \quad (5)$$

where V (cm^3) is the compact volume, r (cm) is the compact radius and h (cm) is the height of the compact.

$$consolidation = (V_b - V_t)/V_b \cdot 100 \quad (6)$$

where V_t (cm^3) is the volume of the compact and V_b (cm^3) is the bulk volume of the powder.

2.2.21. Friability

Approximately 6.5 g of dedusted compacts were weighed precisely using an analytical balance (HR-120, A&D Company, Japan), placed into the plastic drum of a tablet friability tester (FT2, Sotax AG, Switzerland) and rotated at 25 rpm for 4 min in compliance with the Ph. Eur. The dust was then carefully removed and the compacts were reweighed. The percentual loss of the compact mass was calculated for each sample.

2.2.22. Disintegration time

The disintegration test was performed in distilled water at 37.0 ± 2.0 °C on six compacts from each sample using a disintegration test apparatus (ZT 301, Erweka GmbH, Germany). The compacts were considered completely disintegrated when no residue remained in the basket. The results of 6 measurements are expressed as mean values ± standard deviation.

Table 1
Qualitative composition of CPEs.

Components	F-Melt® C	F-Melt® M	F-Melt® F1
Crospovidone	✓	✓	–
D - Mannitol	✓	✓	–
Fujicalin®	✓	–	✓
MCC	✓	✓	✓
Neusilin®	–	✓	–
Waxy rice starch	–	–	✓
Xylitol	✓	✓	–

2.2.23. Determination of wetting time and water absorption ratio

Wetting time and water absorption ratio of the compacts were determined in a Petri dish using a sponge (5 × 5 cm) impregnated with fifteen grams of water containing a water-soluble dye (methylene blue) to facilitate the identification of complete wetting. The tested compact was carefully placed on the surface of the impregnated sponge in the Petri dish at the laboratory temperature. The time required for the solution to reach the upper surface of the compact (T_1) and the time necessary for complete wetting of the compact (wetting time, T_2) by the dye solution were noted. The weight of the compact in the dry state (m_0) and the wetted state (m_1) were measured using the analytical balance. The water absorption ratio (WA) was calculated using the equation:

$$WA = 100 \cdot (m_1 - m_0)/m_0 \quad (7)$$

The results of five measurements are expressed as mean values ± standard deviation.

3. Results and discussion

The evaluated CPEs differ in composition. Only the common substance for all types of F-Melts® is MCC. The F-Melt® C contains taste masking agents D-mannitol and xylitol, crospovidone as a disintegrant and a dibasic calcium phosphate anhydrous (DCPA) known as Fujicalin®. The F-Melt® M has a similar composition as the C type, but the DCPA is replaced by magnesium aluminometasilicate (MAS) available as Neusilin®. Finally, the F-Melt® F1 contains MCC, DCPA and waxy rice starch [31]. The qualitative composition is summarized in Table 1. Initially, all three CPEs were characterized and the compacts were made out of them without any additives. The mixtures and compacts underwent a specific pharmacopoeial and physical evaluation. This article focuses on the comparison of the characteristics relevant to the use of these CPEs for DC.

3.1. Powder flow

The CPEs were evaluated by the methods for pharmaceutical powder flow such as the flow through the orifice, the angle of repose, the angle of slide, Hausner ratio and Carr's index. The *Flow through the orifice* test can simulate flowing of powder through a hopper orifice into the die of tablet compression machine [32]. The powder flow is a critical attribute during tableting [33]. The best flow was measured for sample F1 which can be explained by the spherical shape of its particles (Table 2). According to pharmacopoeial testing of the angle of repose, the sample M exhibited a worse flow (transition from "good" to "fair") in comparison with the C and F1 (characterized as "excellent") (Table 2). Powders, exhibiting such low values in the angle of repose testing (particularly sample C and F1) contribute to ensuring the production of tablets with consistent and reproducible properties such as weight uniformity [34,35].

The regarded result for the *angle of slide* test is 33° [12], which means that there is a prerequisite of a regular flow of the powder from the hopper into tablet matrices. This limit was exceeded by the sample F1 (Table 2), which can be probably related to the smallest mean particle size of the sample due to the higher adhesion of the material to the iron plate of the equipment such as the hopper walls during compression [36]. When the SEM images (Fig. 5A) are compared, it is obvious that the M sample's particles show rather an irregular shape, implying a worse powder flow.

Hausner ratio (HR) and *Carr's index (CI)* were used to compare the powder densification (Table 2) [37].There is a relationship between the HR and sphericity of particles; the HR decreases with the increase of sphericity [38]. This was confirmed, as Fig. 5A shows, that the sample F1 exhibits the best sphericity while having the lowest value of HR. All F-Melts® fit into the range between 1.12 and 1.18 for HR and 11–15 for CI, implying good flow properties. In general, both mobility and density

Table 2
Physical characteristics of CPEs.

Measured value	F-Melt® C	F-Melt® M	F-Melt® F1
Fw [g/s]	16.90 ± 0.11	19.06 ± 0.43	26.14 ± 3.14
Θr [°]	23.22 ± 0.67	35.37 ± 0.98	27.47 ± 0.75
Θs [°]	32.67 ± 0.58	32.67 ± 1.53	34.00 ± 1.73
HR	1.15	1.15	1.12
CI	13.29	13.33	10.96
DB [g/ml]	0.543 ± 0.004	0.562 ± 0.009	0.517 ± 0.007
DT [g/ml]	0.627 ± 0.001	0.648 ± 0.000	0.581 ± 0.005
DP [g/ml]	1.5158 ± 0.0021	1.5301 ± 0.0012	1.5577 ± 0.0036
P [%]	64.5	63.4	66.6
MPS [μm]	156.09	113.79	134.28
D_{10} [μm]	62.54	36.64	40.00
D_{50} [μm]	147.45	105.21	132.15
D_{90} [μm]	261.58	201.73	227.50
SSA [m^2/g]	0.8	4.1	16.0
M [%]	2.093 ± 0.046	1.547 ± 0.138	5.270 ± 0.010
UF_3 [%]	58 ± 0.05	53 ± 0.02	87 ± 0.04
UF_{24} [%]	41 ± 0.12	42 ± 0.04	99 ± 0.01
pH	7.83	7.51	7.44

Fw - flow through the orifice; θr - angle of repose (tg α); θs - angle of slide; HR – Hausner ratio; CI – compressibility index; DB - bulk density; DT - tapped density; DP - pycnometric density; P – porosity; MPS – mean particle size; D_{10}, D_{50}, D_{90} - diameter at which 10, 50 and 90% of the sample's mass is comprised of particles with a diameter less than this value; SSA - specific surface area; M – moisture content; UF_3 - undissolved fraction after 3 min; UF_{24} - undissolved fraction after 24 h; pH (2% solution).

aspects of the flow properties do not differ significantly across the samples.

3.2. Density and porosity of powders

The density of powder is related to the volume of tablets and the dilution potential. Also the position of the punches is influenced by the density of powders, as a lower punch has to be adjusted in a lower position to ensure the same compressing pressure and compact weight, during tableting of less dense substances [39]. The *bulk density (DB)* refers to the mass of powder that can be packed into specific volume. *The tapped density (DT)* is based on collapsing of lose powder into more consolidated state [40]. Measuring of *pycnometric density (DP)* by using helium pycnometer is the closest approximation of the true density [41]. The measured values of bulk density (Table 2) of the C and M correlates with those presented by the manufacturer [42], while the bulk density of the F1 is not stated. Moreover, the densities of all mixtures are very similar (Table 2), which corresponds to similar porosity values and these are probably related to the same method of preparation. The presence of highly porous structure in the tablet matrix is the key factor for rapid disintegration of ODTs [43]. The *porosity of powder* was about 65% in case of all samples (Table 2).

3.3. Particle size and specific surface area

The particle size of the excipients may affect the flow properties and hence the uniformity of the dosage unit [44]. The major components of drug dosage tend to blend better when they are of comparable particle size distribution. Sufficient knowledge of the particle size distribution of excipients helps manufacturers to choose the appropriate particle size of the active substance. When evaluated by sieve analysis, the *mean particle size* decreases in the order of F1 > M > C (Fig. 1A), however the *mean particle size* obtained by laser diffraction showed a different order: C > F1 > M (Table 2, Fig. 1B). Such an irregularity is usually assigned to differences in the principles of the used methods. *The specific surface area* is significantly higher for sample F1 (Table 2), which is related to the particle structure of F1 containing a high amount of surface pores as can be seen in Fig. 5A.

3.4. Moisture content, hygroscopicity, solubility and pH leaching

Wax rice starch is one of the components of the F-Melt® F1, which has a very high percentage of *moisture* (20%) (Table 2) [45], clarifying the decreasing value of moisture in samples in order F1 > C > M.

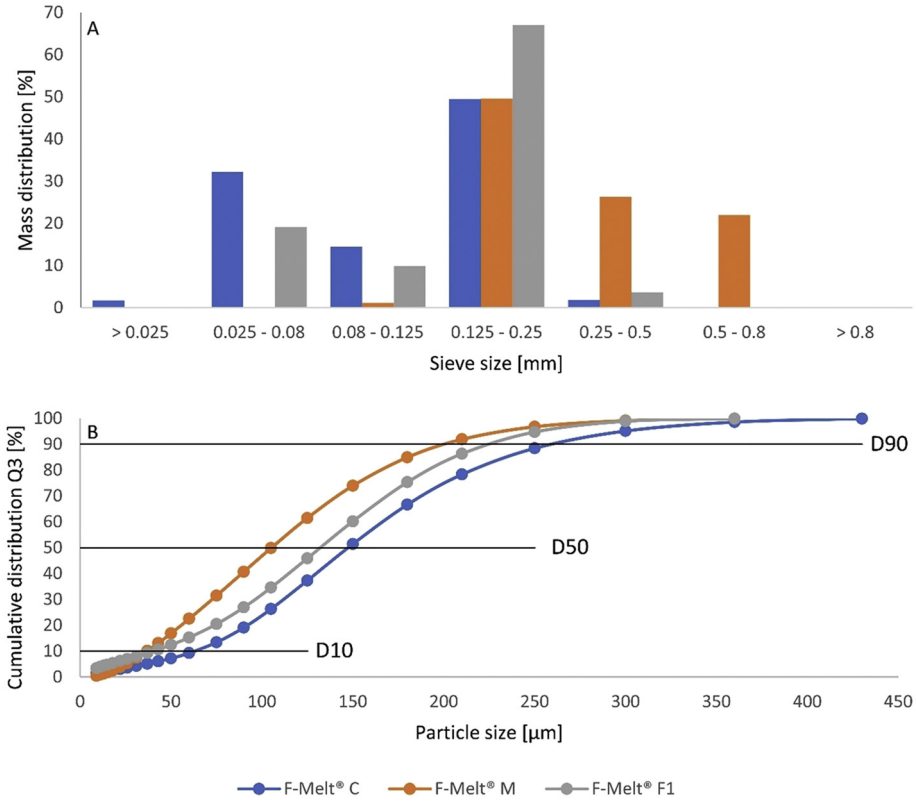

Fig. 1. Particle size distribution by sieve (A) and diffraction analysis (B).

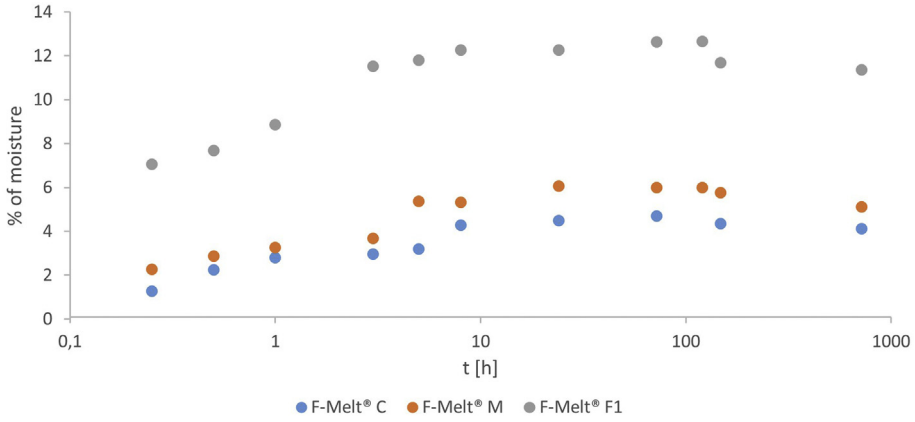

Fig. 2. Hygroscopicity of CPE.

Moreover, samples C and M contain mannitol, as a non-hygroscopic substance [3]. The presence of starch in sample F1 also affected the results of *hygroscopicity* measurement (Fig. 2) The difference in the moisture content between the M and C can be explained by the presence of MAS with good absorption properties [46] in the composition of the M. The *solubility test* simulating the condition in oral cavity showed better solubility of the C and M after 3 min, while the F1 implied the highest percentage of undissolved fraction (Table 2). Therefore, it can be stated that sample F1 may be less suitable for ODTs due to 87% of undissolved fraction, which can cause an unpleasant mouth feeling. The total *undissolved fraction after 24 h* increased in order C < M < F1 (Table 2). Samples C and M had a slightly less undissolved fraction after 24 h than after 3 min. The undissolved fraction in the F1 after 24 h increased in comparison to 3 min. This can be justified by the presence of dibasic calcium phosphate in the F1 types which may create undissolved precipitates in water during a longer time [47].

The pH of the measured CPEs leachates were rated as neutral. Only the C with the pH of 7.83 can be described as slightly basic (Table 2). The neutral pH CPEs can be advantageously combined with different types of APIs and ensure good stability of the product [48].

3.5. Charge density

Throughout manufacturing and handling, interactions occur upon the contact or friction among particles of excipients and APIs, or between the particles and surfaces in contact. These interactions are able to induce electrostatic charge in mixtures - affecting the formulation, manufacturing process and packing behaviour, as well as influencing the mass and content uniformity of the products. For these reasons the *charge density* of excipients was examined. All excipients exhibited increasing negative charge density throughout blending as displayed by Fig. 3. The presence of uncontrolled electrostatic charges may have an adverse effect on powder blend uniformity. In contrast, blending of oppositely charged excipient material and API material can lead to a better blend uniformity. Therefore, all examined excipients may be advantageously blended with positively charged APIs.

Selected properties of CPEs are compared in Fig. 4. The displayed values represent a percentual fraction of the highest value found in each characteristic, to allow an easier comparison. The absolute data are listed in Table 2.

3.6. Scanning electron microscopy (SEM)

All three examined co-processed excipients were manufactured by the means of SpD. This method of preparation usually yields particles with a spherical and regular shape. The only exception arises when fibrous excipients, e.g. cellulose are used, resulting in non-spherical particles. While all examined materials have spherical particles, the sphericity is most prominent in the F1, which comes in the form of big round spheres (Fig. 5A). The plain regular shape of particles of the F1 is probably caused by the presence of starch, present in a form of very fine particles that are easily glued together forming such round shapes.

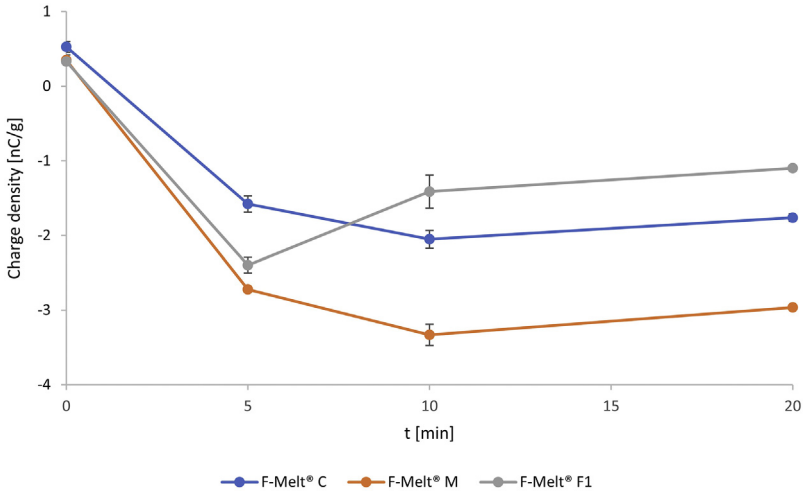

Fig. 3. Charge density throughout blending.

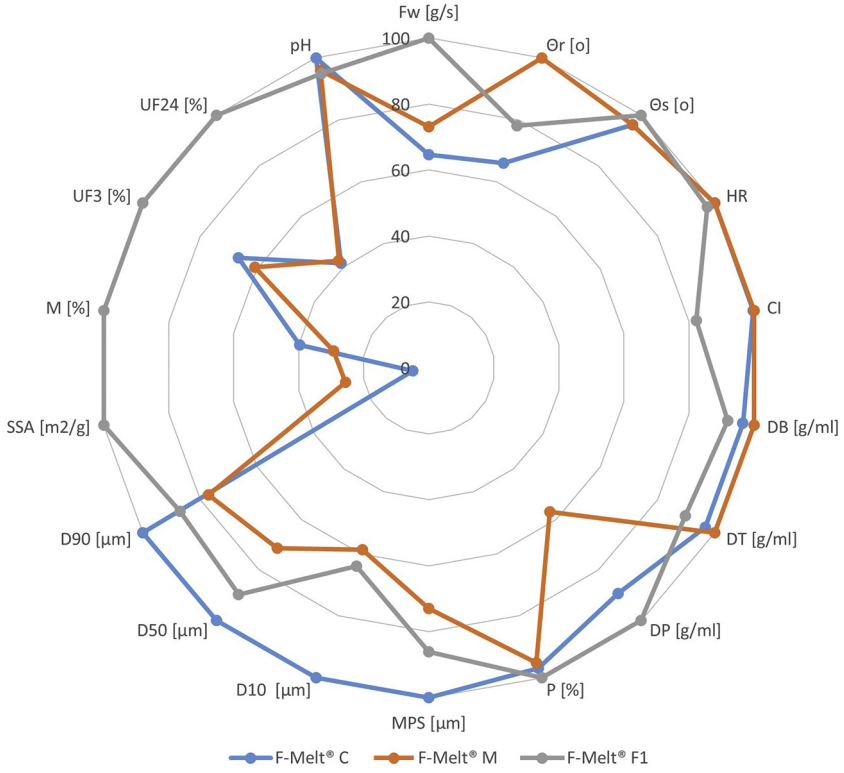

Fig. 4. Physical characteristics of CPEs Fw - flow through the orifice; θr - angle of repose (tg α); CI – compressibility index; DB - bulk density; DT - tapped density; DP - pycnometric density; P – porosity; MPS – mean particle size; D_{10}, D_{50}, D_{90} - diameter at which 10, 50 and 90% of the sample's mass is comprised of particles with a diameter less than this value; SSA - specific surface area; M – moisture content; UF_3 - undissolved fraction after 3 min; UF_{24} - undissolved fraction after 24 h.

The two remaining F-Melt® excipients, C and M, comprise of mannitol, xylitol and MCC. The difference in the excipients causes a slight difference in the look of the primary particles which are rather oval – however, there can be still observed the influence of SpD.

The particles of C are oval and show the most variable size of the primary particles in comparison with the other two F-Melts®. The presence of free mannitol / xylitol particles and also small particles of anhydrous dibasic calcium phosphate can be observed.

The M is similar to the C – it also has free mannitol / xylitol particles. There is also the presence of small particles, but it is probably the MAS in this case. There is a lower content of MCC, which yields slightly less coherent particles and can also have a negative influence on regularity of the shape of the manufactured compacts.

3.7. Differential scanning calorimetry

All the obtained *DSC* curves are displayed in Fig. 6; the curves are stepped by 0.6 W/g. The DSC curve of the F shows no characteristic peaks except for the broad endothermic peak in 50–120 °C region associated with the moisture desorption from starch, MCC and crospovidone. Both the C and M showed peaks corresponding to the presence of crystalline mannitol (peak onset ≈ 165 °C). As the C and M lack typical endotherm of crystalline xylitol melting, it can be concluded that xylitol is present in an amorphous state. Otherwise, there were no specific transitions observed in any of the measured curves, reflecting the fact, that most of the components do not show any even in a pure state.

3.8. Energetic parameters of compression process

The values of all energetic parameters E_{1-3} increased with the rising compression pressure. Out of the energies measured, the highest values were found for *energy* E_1, which is associated with the particles rearrangement, size and shape. For the tested CPEs, the values decreased in the order of F1 > C > M (Table 3). As shown in the Fig. 5A, the particles of the F1 are spherical and of a middle particle size (Table 2), however, their surface is rough. This can lead to a higher friction among the particles during the rearrangement phase and thus to higher values of pre-compression energy. The C and M have particles with a relatively smooth surface and spherical shape. The difference between them can be caused by the particle size distribution. The M particles can easily fill empty spaces during the compression due to their smaller particle size in comparison with the C particles and, therefore, the energy required for the particle rearrangement is lower.

E_2 is the energy consumed for the friction between the particles and the die wall and for the plastic deformation of the particles [27]. The highest values were observed for F1 that contains MCC and starch, both deforming mainly plastically [49,50]. Therefore, interactions like hydrogen bonds or mechanical interlocking can occur among their particles [51]. Furthermore, the plastic energy of the F1 can also be increased

Table 3
Energetic parameters of compression, plasticity and ejection force.

Measured value	CP [MPa]	F-Melt® C	F- Melt® M	F- Melt® F1
E_1 [J]	78	5.19 ± 0.18	5.06 ± 0.17	6.63 ± 0.24
	130	9.76 ± 0.81	10.15 ± 0.46	10.79 ± 0.37
	182	14.88 ± 4.26	13.21 ± 1.02	16.74 ± 0.49
E_2 [J]	78	2.71 ± 0.06	2.80 ± 0.09	3.22 ± 0.07
	130	3.94 ± 0.30	4.00 ± 0.21	4.80 ± 0.18
	182	5.19 ± 0.36	5.33 ± 0.26	5.84 ± 0.18
E_3 [J]	78	0.23 ± 0.00	0.23 ± 0.00	0.27 ± 0.01
	130	0.56 ± 0.02	0.57 ± 0.03	0.64 ± 0.04
	182	1.06 ± 0.04	1.06 ± 0.03	1.17 ± 0.04
PI [%]	78	92.35 ± 0.20	92.54 ± 0.30	92.28 ± 0.26
	130	87.42 ± 1.39	87.54 ± 0.80	88.23 ± 0.65
	182	82.91 ± 1.47	83.45 ± 0.99	83.31 ± 0.82
EF [N]	78	368.52 ± 81.33	405.84 ± 119.71	355.19 ± 97.79
	130	825.93 ± 94.28	494.70 ± 230.75	547.63 ± 17.38
	182	403.88 ± 101.39	677.42 ± 153.55	104.69 ± 38.62

CP – compression pressure; EF-ejection force.

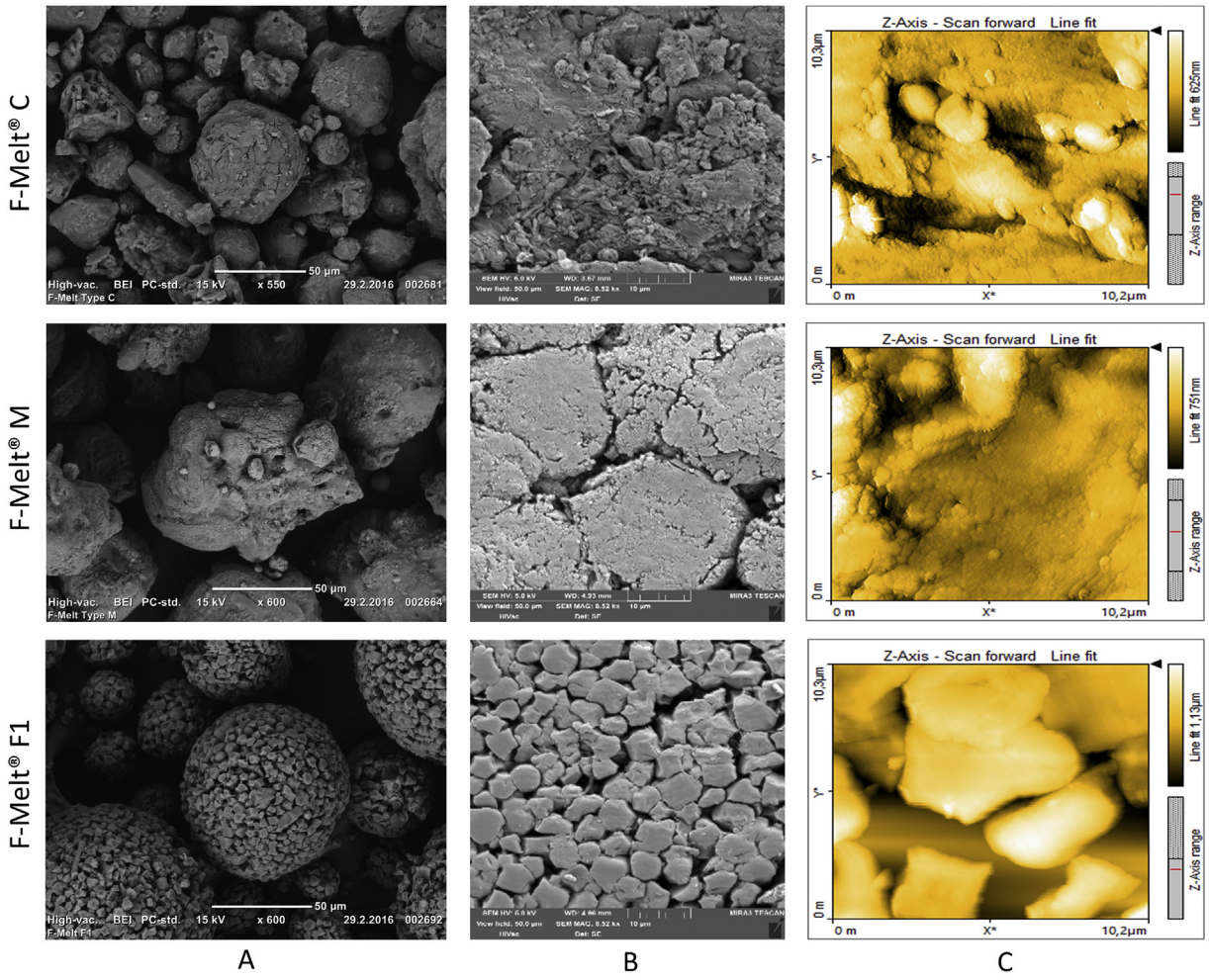

Fig. 5. SEM pictures of (A) CPEs particles (550×, 600×) and (B) compacts compressed at 182 MP (8520×). (C) AFM scans of compacts compressed at 182 MPa.

by the high bonding capacity of starch [52]. The influence of brittle DCPA [53] on the E_2 energy in this formulation (F1) is not significant ($p > 0.05$). In contrast, the lower values of E_2 were found for the M and C (Table 3). The higher energy of the M in comparison to the C can be caused by its smaller particle size [54]. Generally, the smaller particles have more contact areas among themselves and thus more interactions or bonds can be created during the compression process. The difference in the plastic energy of the M and C also reflects in the hardness of the compacts, where the M provides the compacts with a higher tensile strength (Fig. 7B).

Finally, the differences in the elastic *energy* E_3 released during the decompression were compared. Although, the differences were small, the highest values were measured for the F1 again due to the elasticity of the MCC and starch [55]. The stored elastic energy can break bonds during releasing the compression pressure, which results in a lower compact tensile strength of the F1 compacts (Fig. 7B) [56]. The elastic energy of the C and M is of the same value according to the similar composition.

The Pl plasticity values calculated using the Eq. (2) were comparable for all tested samples and decreased with the increasing compression pressure (Table 3). Although the higher values of Pl for the F1 were expected due to its higher values of the plastic energy E_2, its Pl was decreased by the higher elastic energy released after the compression and the values were similar to those of the C and M.

3.9. Ejection force

The ejection force EF was measured as the maximal force needed to eject the compact from the die. The results are shown in Table 3. The M and C exhibited higher values of EF in comparison to the F1. The highest standard deviations were also observed in these materials due to their sticking to the die wall during the compression, which caused the higher experimental data variability. According to Sun [57], the high ejection force is caused by the high residual die wall stress during

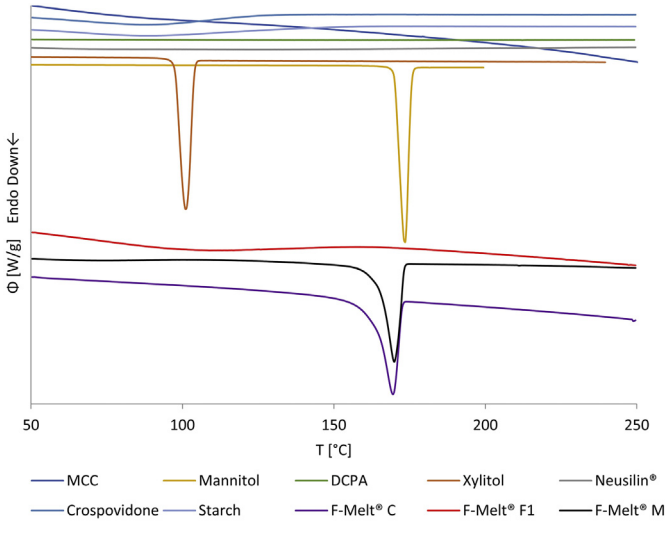

Fig. 6. DSC analysis of components and CPEs.

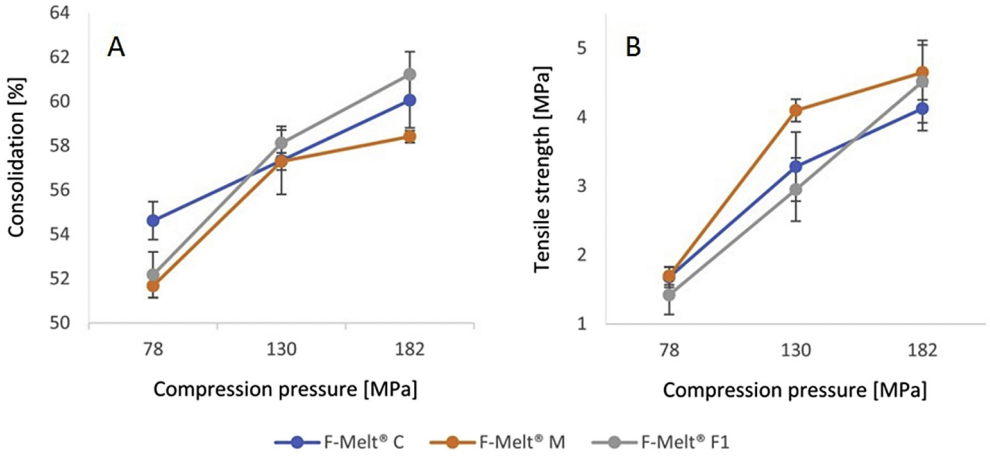

Fig. 7. Consolidation behaviour (A) and tensile strength (B).

the compression, which can increase the frictional force and make the tablet movement more difficult. Abdel-Hamid and Betz [58] presented high values of residual die wall pressure for mannitol, which is one of the main components of the M and C, corresponding with the obtained results. The ejection force for the M increased with the rising compression pressure while the values of EF for C increased from the compression pressure of 78 to 130 MPa and then decreased. A similar decrease in the ejection force at a higher compression pressure was reported by Sun [57] in the case of co-processed MCC and mannitol powder. In opposite, the values of EF for the F1 were lower than those

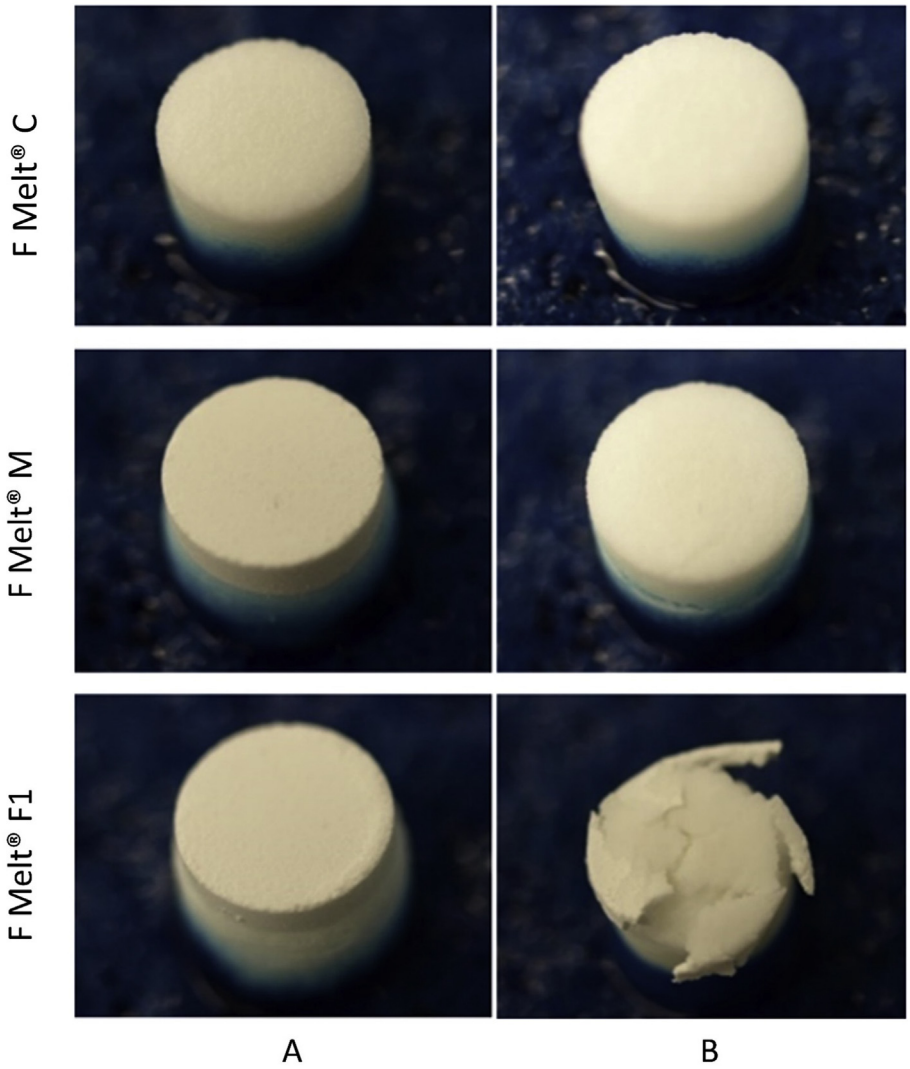

Fig. 8. Compacts compressed at 78 MPa before (A) and after (B) complete wetting.

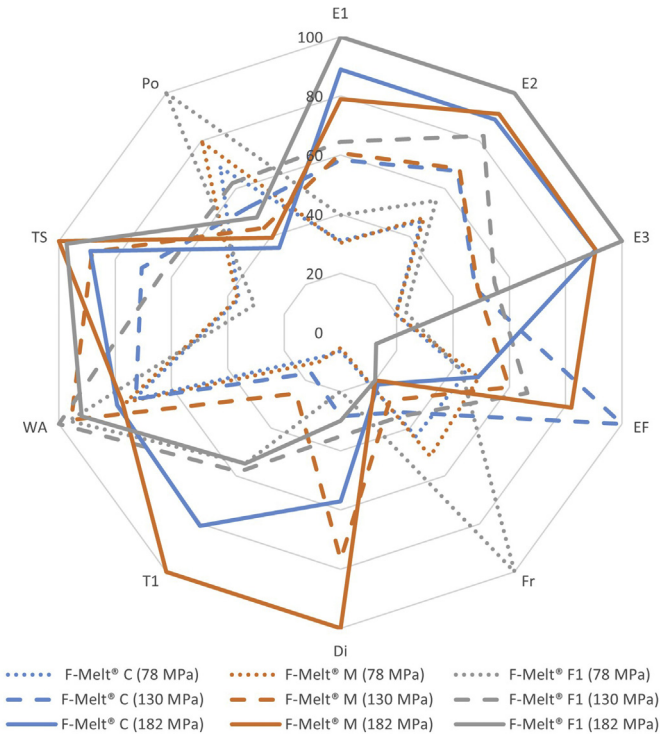

Fig. 9. Energetic parameters and selected properties of compacts; E_{1-3} – energetic parameters; EF – ejection force; Fr - friability; Di - disintegration; T_1, T_2 - wetting time; WA – water absorption ratio; Po – porosity of tablets.

for the M and C thanks to the different composition, in which the MCC and starch imply good self-lubrication properties [59]. However, Abdel-Hamid and Betz [60] stated that viscoelastic materials such as the MCC and starches show a higher adhesion to the die wall and the ejection force than plastic/brittle materials.

3.10. Uniformity of mass

The *uniformity of mass* test was performed to confirm that all compacts were compressed at a similar compaction condition, as each compact was prepared individually using the Zwick/Roell T1-FRO 50 machine without the automatic filling of the die. The evaluation of the weight variation showed that all the compacts fulfil the requirements given by the Ph. Eur. [61](Table 4). However, considering the differences in flow properties of all the samples (Table 2), the deterioration of mass uniformity might be expected when no glidants or lubricants are used.

Moreover, it was observed that the compacts containing the F1 and M have a higher average weight than the compacts containing the C, although, the starting mass of the material was the same (200 ± 1 mg). This may be caused by the presence of MAS and starch in the composition of these F-Melt® types. These excipients are good absorbents and therefore may absorb air humidity and hence increase the weight of tablets during the storage [62]. According to this observation, it can be stated that the F1 and M are more suitable for the incorporation of moisture-sensitive ingredients as they can protect these substances by bonding water in their porous structure [63].

3.11. AFM imaging

The *AFM imaging* was carried out to measure the surface topography and also the surface roughness (Sq) of the M, C and F1 compacts. These parameters can describe and characterize the surface [64] and are important for the particle-particle interactions, the absorption of liquids (e.g. dissolution medium) or adherence of tablets coatings [65]. The AFM imaging is in this case more suitable for describing the tablets surface than the SEM as it can provide quantitative information about any irregularities.

Table 4
Properties of compacts.

Measured Value	CP [MPa]	F- Melt® C	F- Melt® M	F- Melt® F1
UM [mg]	78	201.03 ± 0.26	201.04 ± 0.25	202.86 ± 0.74
	130	200.85 ± 0.57	202.42 ± 0.36	206.38 ± 0.85
	182	200.42 ± 0.19	200.26 ± 036	200.47 ± 0.25
Sq [nm]	78	–	–	–
	130	–	–	–
	182	165.01 ± 77.17	150.75 ± 66.37	241.23 ± 50.38
PD [g/cm^3]	78	1.4989 ± 0.0003	1.4994 ± 0.0003	1.5336 ± 0.0002
	130	1.4985 ± 0.0001	1.4936 ± 0.0002	1.5373 ± 0.0001
	182	1.5042 ± 0.0003	1.5037 ± 0.0001	1.5420 ± 0.0005
Po [%]	78	20.6	23.8	29.9
	130	15.7	13.1	18.6
	182	10.6	11.8	14.4
He [mm]	78	4.31 ± 0.07	4.44 ± 0.04	4.76 ± 0.07
	130	4.07 ± 0.14	3.97 ± 0.01	4.20 ± 0.05
	182	3.87 ± 0.11	3.90 ± 0.02	3.93 ± 0.08
Fr [%]	78	0.26	0.31	0.60
	130	0.20	0.17	0.21
	182	0.13	0.12	0.12
Di [min]	78	0.21 ± 0.10	0.17 ± 0.05	0.65 ± 0.13
	130	0.93 ± 0.12	2.52 ± 0.42	1.15 ± 0.37
	182	1.87 ± 0.33	3.28 ± 0.83	0.98 ± 0.28
T_1 [min]	78	0.18 ± 0.05	0.22 ± 0.07	0.97 ± 0.05
	130	0.30 ± 0.05	0.45 ± 0.12	1.03 ± 0.17
	182	1.43 ± 0.98	1.77 ± 0.72	0.97 ± 0.63
T_2 [min]	78	0.28 ± 0.05	0.30 ± 0.08	2.45 ± 0.52
	130	0.50 ± 0.07	0.70 ± 0.13	2.22 ± 1.02
	182	1.97 ± 1.25	2.25 ± 0.78	2.80 ± 2.03
WA [%]	78	90.77 ± 4.92	94.31 ± 6.31	119.29 ± 8.82
	130	89.96 ± 2.94	118.29 ± 6.93	123.65 ± 10.89
	182	98.06 ± 21.30	95.68 ± 14.79	113.58 ± 11.66

CP - compression pressure; UM - uniformity of mass; Sq – surface roughness; PD - pycnometric density; Po – porosity of tablets; He - height; Fr - friability; Di - disintegration; T_1, T_2 - wetting time; WA – water absorption ratio.

The values of *Sq* are listed in Table 4. The highest roughness was observed in the F1 compacts. As can be seen in Fig. 5B and C, the particles forming the compact are not in a close contact and there is a large amount of surface pores between them. These pores and the arrangement of the individual particles of the excipients forming the F1 increase the roughness of the final compact. The *Sq* values for the M and C were similar while the slightly higher values of the C are caused by the presence of small fragments of the material on the surface of its compacts. As a result, there is a larger range of the distances between the highest and lowest points and therefore the expressed roughness is slightly higher. In the case of M, the surface of the compressed and deformed particles is smoother and the irregularities occur mainly at the areas of the particle contact.

3.12. Pycnometric density and porosity of the compact

The evaluation of the compacts' *pycnometric density* revealed that in all three materials the density increases with the increasing compression pressure. However, in the case of the C and M, the increase in the density between the pressure of 78 and 130 MPa is negligible. Moreover, these two materials imply almost the same values of the pycnometric density, which is caused by their similar composition.

The greatest increase and simultaneously the highest values of pycnometric density were observed in the F1 compacts. This increase in the pycnometric density may be explained in two different ways. First of them is related to the lower height of the compacts and hence their decreasing volumes, while the surface pores are nearly negligible. The other possible explanation lies in the greater amount of the surface pores accessible for the helium, while not being a part of the overall compact volume.

According to the obtained results from the evaluation of the compact height (Table 4), it can be stated that the increasing pycnometric density in the case of the C and M is connected to the decrease of the compact height. On the other hand, the higher values of density in all compacts containing the F1 are presumably caused by the porosity of the compacts as can be also seen in Fig. 5B. This assumption was also confirmed by the calculation of the *compact porosity* (Table 4) and by the AFM measurement as already discussed above. Moreover, this explanation is supported by the results of disintegration and wetting evaluations where the F1 implied fast disintegration and wetting. The increase in pycnometric density of all compacts with the increasing compression pressure may be explained by the decrease in the compact height and volume.

3.13. Compact height and consolidation behaviour

The decrease in the *compacts' height* with the increasing compression pressure was observed in all three F-Melt® types as could be seen in Table 4. The height of the compacts containing different types of F-Melt® was in the order of C < M < F1 with the exception in the pressure of 130 where the height increase in the order of M < C < F1. Compressing of the F1 leads in all three pressure settings to the highest compacts with the greatest porosity (Table 4). This observation may be related to the highest values of the E_1 energy that is connected to the particles rearrangement. The particles of F1 put up a higher resistance during the compression yielding higher and more porous compacts. On the other hand, the E_1 energies of the M and C are similar and smaller in comparison to the F1 resulting in lower and less porous compacts.

The degree of *consolidation* was in the order of M < C < F1, except for the pressure of 78 MPa, where the greatest consolidation was observed in the C. The highest loss of volume during the compression showed the F1 (Fig. 7A), corresponding to the lowest value of CI (Table 2). This observation may be caused by a higher content of air in the co-processed particles of the F1, which is squeezed out during the compression. Moreover, the spherical particles of the F1 are deformed and their fragments are rearranged which can also cause the loss in the compacts' volume/height. This material also showed the highest decrease in the compact height (17.4%) observed for the compacts prepared, using the compression pressure of 78 and 182 MPa. On the other hand, the lowest decrease in the compact height (10.2%) was observed in the C, which simultaneously implied linear consolidation behaviour at the used range of compression pressures. This observation also corresponds to the calculated values of compacts porosity which was in the order of C < M < F1.

3.14. Tensile strength of compacts

The results of the calculated *tensile strength* of the compacts are shown in Fig. 7B. As can be seen, the tensile strength of all compacts rises with the increasing compression pressure as expected. Mechanical resistance of the compacts increases in the order of F1 < C < M.

The highest values were observed for the M. This can be caused by the combination of brittle, plastic (mannitol, xylitol, DCPA) and viscoelastic (MCC) excipients in the co-processed product. Brittle materials fragment during the compression process and create new surfaces for bonding while plastic and viscoelastic materials provide good bonding properties, without creating new surfaces. Therefore these materials are usually more lubricant-sensitive [66,67] and the deterioration of the M compact hardness can be expected when lubricants are used.

The lower values were found for the C due to the different particle size and the content of DCPA instead of MAS. The DCPA is considered a brittle material and new surfaces are available as bonding areas. Nevertheless, low values of tensile strength of the compacts prepared using low compression pressure are caused by the inferior plastic deformation of brittle and plastic materials [68]. The tensile strength of C also corresponds to its lower plastic energy of the E_2 obtained from the force-displacement record (Table 3). Similar results were observed also by Brniak et al. [22]. To the opposite, in the study of Krupa et al. [21], in which tablets containing the C and M were prepared, a lower tensile strength for the M was measured. This can be caused by the presence of a lubricant (sodium stearate fumarate) in their mixtures. This observation also supports the assumption that the M is more lubricant sensitive as mentioned above.

The lowest values of tensile strength (except of the compression pressure of 182 MPa) were estimated for the F1 compacts, although its plastic energy E_2 was the highest. However, the tensile strength is influenced by the elastic energy E_3 released from the compact after the compression. The F1 exhibit the highest E_3 which can decrease the tensile strength by the relaxation of the compacts and reduce the interactions among particles [56,69]. Moreover, a linear relationship of the tensile strength on the compression pressure can be observed in the measured range of pressures for F1.

3.15. Friability

All prepared compacts fulfil the requirements given by the Ph. Eur. for the *friability* testing [61] as can be seen in Table 4. In all three samples, a decrease in friability was observed with an increment in the compression pressure that also correlates with the increase in the compact hardness (tensile strength). Similar results were observed by Brniak et al. [19]. In their study, tablets containing C were prepared at three different compression forces of 10, 15 and 20 kN (88.4, 132.6 and 176.8 MPa). These tablets also implied friability lower than 1% and the value decreased with the increasing compression force.

The values of friability at the compression pressure of 78 MPa were in the order of C < M < F1. Also Krupa et al. [21] stated that the tablets containing the M in the combination with 2% of sodium stearyl fumarate exhibited a higher friability than tablets containing the C in a combination with 2% of sodium stearyl fumarate. However, in general, the values obtained by Brniak et al. [19] and Krupa et al. [21] were slightly higher in comparison to the values obtained in this study.

The highest value of friability in the F1 compacts may be caused by the presence of interparticle spaces and less contact areas for bonding, which can be seen in Fig. 5B and 4C. The high amount of pores leads to a lower particles cohesion and hence to a higher friability value.

3.16. Disintegration time

The *disintegration times* of all prepared compacts are presented in Table 4. Except for the compacts containing the M prepared at 182 MPa, all the obtained compacts fulfilled the requirements of the Ph. Eur. [61] for fast disintegrating tablets (<3 min), while the compacts compressed at 78 MPa from the C and M also met the recommendation of FDA (<30 s) [70]. Moreover, the evaluation of the disintegration time revealed that increasing compression pressure leads to compacts with prolonged disintegration time with the only exception for the F1 compacts, where the differences in the disintegration times between the pressures of 130 and 182 MPa were statistically insignificant ($p > 0.05$). The prolongation of the disintegration times with the higher compression pressure may be explained by lower porosity of the compacts that leads to a decrease in the water penetration into the compacts. These results also correspond with the increasing values of the tensile strength (Fig. 7B), which very often leads to a slower disintegration due to the stronger interparticle bonds [71,72].

The slowest disintegration was expected in the F1 compacts as the M and C contain superdisintegrant crospovidone. However, the disintegration rate differs depending on the used compression pressure and CPE (Table 4).

The fast disintegration of the F1 compacts compressed at higher pressures can be explained by the presence of starch in this co-processed material. The original assumption was that starches disintegrate the compact structure due to the swelling action [73]. However,

there were several studies [74,75] that suggested another mechanism of their action such as repulsion, deformation or penetration. Lowenthal [76] claimed that starch grains are deformed during compression and do not regain their original shape when moistened with water. Nevertheless, it was also observed that the tighter arrangement, the greater is the disruption. Similar observations were published also by Hill [77] and these are in compliance with the results of this study, where the disintegration of the compacts prepared at 182 MPa are similar to those compressed at 130 MPa. Moreover, the F1 contains also MCC and DCPA, which both enhance the transport of liquid into a compact matrix [3,72].

The C and M compacts compressed at 78 MPa had similar disintegration rates as was expected according to their similar composition. However, the disintegration of the compacts prepared using higher pressures differs significantly ($p < 0.05$). Similar differences in the disintegration times of the compacts containing the C and M were observed by Krupa et al. [21]. The faster disintegration of the C is probably caused by the presence of DCPA, which allows the complete penetration of the liquid into the compacts due to its hydrophilic nature [3]. The greater penetration of water caused faster action of the superdisintegrant crospovidone. This assumption also correlates with the results from the evaluation of the compacts' wetting times that are discussed below. On the other hand, it is well known that MAS can retain high amounts of liquids in its porous structure [13]. Therefore, its presence in the composition of the M can cause the retention of water, leading to the deceleration of the disintegration process.

3.17. Wetting time and water absorption ratio

The results from the determination of *wetting times* and *water absorption ratio WA* are listed in Table 4. Both the wetting times and absorption ratio of the compacts increased in the order C < M < F1. Generally, the wetting times closely relate to the hydrophilicity of the excipients and to the inner structure of the compacts. Its values usually increase with the lower porosity, smaller size of pores and increase in compression pressure. The negative effect of the compression pressure on wetting times was observed in the compacts containing the C and M. In the case of the F1 compacts, the wetting times were similar in all three pressures ($p > 0.05$). This observation can be explained by the presence of DCPA in combination with starch. The DCPA causes fast penetration of water into the compacts, while the starch grains are moisturized and start to disintegrate the compacts during the wettability measurements as can be seen in Fig. 8A and B. The early disruptions of the compacts reduce the contact surfaces and penetration of water to the upper parts of the compact is slower. The F1 compacts also implied the highest values of the absorption ratio. This observation indicates gentle swelling of starch, which results in a higher weight of the wetted compacts.

The wetting times of the C and M compacts are comparable, but wetting of the C compacts is slightly faster in comparison to the M compacts, which is probably caused by the penetration enhancing properties of the DCPA already described above. Similar results were described by Krupa et al. [21]. In their study, the wetting time of the placebo compacts prepared at 88.4 MPa containing the C was about 1 min, while the wetting time of the M compacts was about 2 min. These values are slightly higher in comparison to the results obtained in this study, which can be caused by the presence of lubricant sodium stearyl fumarate.

The values of WA of the C compacts were lower in comparison to the M compacts and similar to those obtained by Brniak et al. [22]. The higher values of water absorption ratio of the M compacts can be caused by the absorption properties of MAS, which retains water in its porous structure and hence increases the weight of the wetted compacts. It can be seen in Fig. 8B, that the compacts containing the M exhibited slight swelling. According to this observation, it can be deduced that the composition of the M and C differs not only in the presence of the DCPA and MAS, but also in the percentage representation of swelling excipients, such as crospovidone and MCC.

Fig. 9 comprehensively sums selected properties of the compacts in relation to the compression pressure and CPE. The values are displayed as a percentual fraction of the highest found value – the absolute data can be retrieved from Tables 3 and 4.

4. Conclusion

The three novel co-processed excipients F-Melts® and the compressed compacts without any other excipients or API were comprehensively evaluated in the mean of their physical properties. All the tested excipients are prepared by the spray drying technique and are suitable for the direct compression. The types C and M are intended for pharmaceutical preparations, while the C and F1 for the nutraceutical ones. In general, it could be stated that the C and M have very similar properties according to their similar composition, while the properties of the F1 mostly differ significantly. The C implies excellent to good flow properties, contains mid-size spherical particles, and shows the lowest hygroscopicity, growing negative charge, poor lubricity, intermediate tensile strength and disintegration time. The M possessed good flow properties, large spherical particles, low hygroscopicity, the most growing negative charge, poor lubricity, the highest tensile strength and the slowest disintegration of the compacts. The F-Melt® M is more convenient for the incorporation of the moisture sensitive ingredients according to the presence of magnesium aluminometasilicate in its composition. The F1 shows excellent to good flow properties, small spherical particles with the highest specific surface area and hygroscopicity, its charge fluctuates throughout blending. It also exhibits poor lubricity, middle-range linearly growing tensile strength and fast disintegration of the compacts. Similarly to the M, the F1 is also suitable for the incorporation of moisture sensitive ingredients as it contains starch and magnesium aluminometasilicate.

In general, it is difficult to select the best CPE as they possess different properties fitting the versatile needs of manufacturers. According to the obtained results it can be stated that all three types of the F-Melt® excipients possessed sufficient flow properties, spherical particles and poor lubricity. Their compression leads to compacts with high tensile strength, low friability and fast disintegration and therefore they are suitable for the preparation of orodispersible tablets containing pharmaceutical or nutraceutical ingredients by direct compression.

Declaration of Competing Interest

The authors report no conflict of interest. The authors alone are responsible for the content and writing of this article.

Acknowledgements

References

[1] J. Klancke, Dissolution testing of orally disintegrating tablets, Dissolution Technol. 10 (2003) 6–8.
[2] A.A. Ali, N.A. Charoo, D.B. Abdallah, Pediatric drug development: formulation considerations, Drug Dev. Ind. Pharm. 40 (10) (Oct. 2014) 1283–1299.
[3] Martini Jivraj, Thomson, An overview of the different excipients useful for the direct compression of tablets, Pharm. Sci. Technol. Today 3 (2) (Feb. 2000) 58–63.
[4] D. McCormick, Evolutions in direct compression, Pharm. Technol. 29 (April) (2005) 52–62.
[5] R. Adamek, M. Řehula, T. Rysl, Chemical structure and viscoelasticity of fillers for direct compression of drug tablets, Chem. List. 105 (9) (2011) 691–696.
[6] A. Franc, D. Vetchý, P. Vodáčková, R. Kubalák, L. Jendryková, R. Goněc, Co-processed excipients for direct compression of tablets, Čes. slov. Farm. 67 (2018) 143–153.
[7] S.K. Nachaegari, A.K. Bansal, Coprocesed excipients for solid dosage form, Pharm. Technol (2004) 52–64.
[8] S.A. Tayel, M.A. El Nabarawi, M.M. Amin, M.H.H. AbouGhaly, Comparative study between different ready-made orally disintegrating platforms for the formulation of Sumatriptan succinate sublingual tablets, AAPS PharmSciTech 18 (2) (Feb. 2017) 410–423.
[9] T. Nobukazu, N. Yoshiro, K. Hiroshi, F. Tadashi, H. Terumasa, Composition for rapid disintegrating tablet in oral cavity, EP 1 523 974 A1, 2004.

[10] "Discover new ways to improve ODT performance with Fuji F-MELT® system." [Online]. Available: www.fujichemical.co.jp%7Cpharma@fujichemical.co.jp. [Accessed: 31-Oct-2018].
[11] Ltd., Fuji. F-Melt: Fujis futuristic excipient system, [Online]. Available https://www.yumpu.com/en/document/view/2791410/f-meltr-type-c-and-f1-harke-group/5, Accessed date: 31 October 2018.
[12] B. Vraníková, J. Gajdziok, Liquisolid systems and aspects influencing their research and development, Acta Pharma. 63 (4) (2013) 447–465.
[13] B. Vraníková, J. Gajdziok, D. Vetchý, Determination of flowable liquid retention potential of aluminometasilicate carrier for liquisolid systems preparation, Pharm. Dev. Technol. 20 (7) (Oct. 2015) 839–844.
[14] M.J. Kang, et al., Immediate release of ibuprofen from Fujicalin ® -based fast-dissolving self-emulsifying tablets, Drug Dev. Ind. Pharm. 37 (11) (Nov. 2011) 1298–1305.
[15] H. Schlack, A. Bauer-Brandl, R. Schubert, D. Becker, Properties of Fujicalin®, a new modified anhydrous dibasic calcium phosphate for direct compression: comparison with Dicalcium phosphate Dihydrate, Drug Dev. Ind. Pharm. 27 (8) (Jan. 2001) 789–801.
[16] F-MELT Directly Compressible Excipient System for Fast-Disintegrating Oral Tablets, [Online]. Available http://www.fujichemical.co.jp/english/newsletter/newsletter_pharma_0802.html, Accessed date: 31 October 2018.
[17] S.H. Curry, Translational science: past, present, and future, Biotechniques 44 (2S) (Feb. 2008) ii–viii.
[18] M. Gibson, Pharmaceutical preformulation and formulation : a practical guide from candidate drug selection to commercial dosage form, Boca Raton: Informa Healthcare, 2009.
[19] W. Brniak, R. Jachowicz, A. Krupa, T. Skorka, K. Niwinski, Evaluation of co-processed excipients used for direct compression of orally disintegrating tablets (ODT) using novel disintegration apparatus, Pharm. Dev. Technol. 18 (2) (Apr. 2013) 464–474.
[20] M. Köllmer, C. Popescu, P. Manda, L. Zhou, R.A. Gemeinhart, Stability of benzocaine formulated in commercial Oral disintegrating tablet platforms, AAPS PharmSciTech 14 (4) (Dec. 2013) 1333–1340.
[21] A. Krupa, R. Jachowicz, Z. Pędzich, K. Wodnicka, The influence of the API properties on the ODTs manufacturing from co-processed excipient systems, AAPS PharmSciTech 13 (4) (Dec. 2012) 1120–1129.
[22] W. Brniak, R. Jachowicz, P. Pelka, The practical approach to the evaluation of methods used to determine the disintegration time of orally disintegrating tablets (ODTs), Saudi Pharm. J. SPJ Off. Publ. Saudi Pharm. Soc. 23 (4) (Sep. 2015) 437–443.
[23] Y. Gonnissen, J.P. Remon, C. Vervaet, Development of directly compressible powders via co-spray drying, Eur. J. Pharm. Biopharm. 67 (1) (Aug. 2007) 220–226.
[24] B. Vraníková, J. Gajdziok, D. Vetchý, Modern evaluation of liquisolid systems with varying amounts of liquid phase prepared using two different methods, Biomed. Res. Int. 2015 (May 2015), 608435.
[25] S. Brunauer, P.H. Emmett, E. Teller, Adsorption of gases in multimolecular layers, J. Am. Chem. Soc. 60 (2) (Feb. 1938) 309–319.
[26] D. Hobbs, J. Karagianis, T. Treuer, J. Raskin, An in vitro analysis of disintegration times of different formulations of olanzapine orodispersible tablet: a preliminary report, Drugs R. D. 13 (4) (Dec. 2013) 281–288.
[27] A. Fahr, Voigt Pharmazeutische Technologie, Dtsch. Apotheker Verlag, 2015 468.
[28] 7-16 STAMM, A. and C. MATHIS, Verpressbarkeit von Festen Hilfsstoffen für Direkttablettierung, Acta Pharmaceutica Technologica, 1976 22, No Title.
[29] G. E. Amidon, P. J. Secreast, and D. Mudie, "Chapter 8 - Particle, Powder, and Compact Characterization," Y. Qiu, Y. Chen, G. G. Z. Zhang, L. Liu, and W. R. B. T.-D. S. O. D. F. Porter, Eds. San Diego: Academic Press, 2009, pp. 163–186.
[30] J.T. Fell, J.M. Newton, Determination of tablet strength by the Diametral-compression test, J. Pharm. Sci. 59 (5) (May 1970) 688–691.
[31] V.A. Saharan, Current Advances in Drug Delivery through Fast Dissolving/Disintegrating Dosage Forms, Bentham Science Publishers, 2017.
[32] I.. Sinka, L.C.. Schneider, A.C. Cocks, Measurement of the flow properties of powders with special reference to die fill, Int. J. Pharm. 280 (1–2) (Aug. 2004) 27–38.
[33] H. Hurychová, M. Kuentz, Z. Šklubalová, Fractal aspects of static and dynamic flow properties of pharmaceutical excipients, J. Pharm. Innov. 13 (1) (Mar. 2018) 15–26.
[34] A. Crouter, L. Briens, The effect of moisture on the Flowability of pharmaceutical excipients, AAPS PharmSciTech 15 (1) (Feb. 2014) 65–74.
[35] A.R. Fassihi, I. Kanfer, Effect of compressibility and powder flow properties on tablet weight variation, Drug Dev. Ind. Pharm. 12 (11–13) (Jan. 1986) 1947–1966.
[36] M.G. Herting, P. Kleinebudde, Roll compaction/dry granulation: effect of raw material particle size on granule and tablet properties, Int. J. Pharm. 338 (1–2) (Jun. 2007) 110–118.
[37] R.B. Shah, M.A. Tawakkul, M.A. Khan, Comparative evaluation of flow for pharmaceutical powders and granules, AAPS PharmSciTech 9 (1) (Mar. 2008) 250–258.
[38] R.P. Zou, A.B. Yu, Evaluation of the packing characteristics of mono-sized non-spherical particles, Powder Technol. 88 (1) (Jul. 1996) 71–79.
[39] Y. Yamamoto, et al., Effect of powder characteristics on oral tablet disintegration, Int. J. Pharm. 365 (1–2) (Jan. 2009) 116–120.
[40] E.C. Abdullah, D. Geldart, The use of bulk density measurements as flowability indicators, Powder Technol. 102 (1999) 151–165.
[41] M. Viana, P. Jouannin, C. Pontier, D. Chulia, About pycnometric density measurements, Talanta 57 (3) (May 2002) 583–593.
[42] f-melt.com, , [Online]. Available http://www.f-melt.com/product/general_properties.php, Accessed date: 31 October 2018.
[43] S. Bandari, R.K. Mittapalli, R. Gannu, Orodispersible tablets: an overview, Asian J. Pharm. Free full text Artic. Asian J. Pharm. 2 (1) (Aug. 2014).
[44] B.R. Rohrs, G.E. Amidon, R.H. Meury, P.J. Secreast, H.M. King, C.J. Skoug, Particle size limits to meet USP content uniformity criteria for tablets and capsules, J. Pharm. Sci. 95 (5) (May 2006) 1049–1059.
[45] A.K. Anderson, H.S. Guraya, Effects of microwave heat-moisture treatment on properties of waxy and non-waxy rice starches, Food Chem. 97 (2) (2006) 318–323.
[46] B. Vraníková, J. Gajdziok, Evaluation of sorptive properties of various carriers and coating materials for liquisolid systems, Acta Pol. Pharm. 72 (3) (2015) 539–549.
[47] L.D. Eggert, W.J. Rusho, M.W. MacKay, G.M. Chan, Calcium and phosphorus compatibility in parental nutrition solutions for neonates, Am. J. Hosp. Pharm. 39 (1) (Jan. 1982) 49–53.
[48] A.S. Narang, D. Desai, S. Badawy, Impact of excipient interactions on solid dosage form stability, Pharm. Res. 29 (10) (Oct. 2012) 2660–2683.
[49] E. Doelker, Comparative compaction properties of various microcrystalline cellulose types and generic products, Drug Dev. Ind. Pharm. 19 (17–18) (Jan. 1993) 2399–2471.
[50] Y. Zhang, Y. Law, S. Chakrabarti, Physical properties and compact analysis of commonly used direct compression binders, AAPS PharmSciTech 4 (4) (Dec. 2003) E62.
[51] C. Nyström, Gör. Alderborn, M. Duberg, P.-G. Karehill, Bonding surface area and bonding mechanism-two important factors fir the understanding of powder comparability, Drug Dev. Ind. Pharm. 19 (17–18) (Jan. 1993) 2143–2196.
[52] C.-Y. Wu, S.M. Best, A.C. Bentham, B.C. Hancock, W. Bonfield, A simple predictive model for the tensile strength of binary tablets, Eur. J. Pharm. Sci. 25 (2005) 331–336.
[53] C.K. Tye, C. (Calvin) Sun, G.E. Amidon, Evaluation of the effects of tableting speed on the relationships between compaction pressure, tablet tensile strength, and tablet solid fraction, J. Pharm. Sci. 94 (3) (Mar. 2005) 465–472.
[54] A. McKenna, D.F. McCafferty, Effect of particle size on the compaction mechanism and tensile strength of tablets, J. Pharm. Pharmacol. 34 (6) (Jun. 1982) 347–351.
[55] O. Antikainen, J. Yliruusi, Determining the compression behaviour of pharmaceutical powders from the force-distance compression profile, Int. J. Pharm. 252 (1–2) (Feb. 2003) 253–261.
[56] K.V. Maarschalk, H. Vromans, G.K. Bolhuis, C.F. Lerk, The effect of viscoelasticity and tabletting speed on consolidation and relaxation of a viscoelastic material, Eur. J. Pharm. Biopharm. 42 (1) (Jan-1996) 49–55.
[57] C.C. Sun, Dependence of ejection force on tableting speed—a compaction simulation study, Powder Technol. 279 (Jul. 2015) 123–126.
[58] S. Abdel-Hamid, G. Betz, Study of radial die-wall pressure changes during pharmaceutical powder compaction, Drug Dev. Ind. Pharm. 37 (4) (Apr. 2011) 387–395.
[59] L.H. Han, J.A. Elliott, A.C. Bentham, A. Mills, G.E. Amidon, B.C. Hancock, A modified Drucker-Prager cap model for die compaction simulation of pharmaceutical powders, Int. J. Solids Struct. 45 (10) (May 2008) 3088–3106.
[60] S. Abdel-Hamid, G. Betz, A novel tool for the prediction of tablet sticking during high speed compaction, Pharm. Dev. Technol. 17 (6) (Dec. 2012) 747–754.
[61] Český lékopis 2005 : (ČL 2005) = Pharmacopea bohemica MMV : (Ph. B. MMV). , Grada, Praha, 2005.
[62] R.C. Rowe, P.J. Sheskey, S.C. Owen, American Pharmacists Association, Handbook of Pharmaceutical Excipients, 6th ed APhA/Pharmaceutical Press, London, Chicago, 2009.
[63] S. Bharate, S. Bharate, A. Bajaj, Interactions and incompatibilities of pharmaceutical excipients with active pharmaceutical ingredients: a comprehensive review, J. Excipients Food Chem. 1 (3) (2010) 3–26.
[64] J.D. Kiely, D.A. Bonnell, Quantification of topographic structure by scanning probe microscopy, J. Vac. Sci. Technol. B Microelectron. Nanom. Struct. Process. Meas. Phenom. 15 (4) (Jun. 1998) 1483.
[65] P. Seitavuopio, J. Rantanen, J. Yliruusi, Tablet surface characterisation by various imaging techniques, Int. J. Pharm. 254 (2) (Mar. 2003) 281–286.
[66] L.L. Augsburger, S.W. Hoag, Pharmaceutical Dosage Forms - Tablets : Rational Design and Formulation, Informa Healthcare, 2008.
[67] S. Saha, A.F. Shahiwala, Multifunctional coprocessed excipients for improved tabletting performance, Expert Opin. Drug Deliv. 6 (2) (Feb. 2009) 197–208.
[68] C.C. Sun, Decoding powder tabletability: roles of particle adhesion and plasticity, J. Adhes. Sci. Technol. 25 (4–5) (Jan. 2011) 483–499.
[69] K. Zuurman, K. Van der Voort Maarschalk, G.K. Bolhuis, Effect of magnesium stearate on bonding and porosity expansion of tablets produced from materials with different consolidation properties, Int. J. Pharm. 179 (1) (Mar. 1999) 107–115.
[70] Guidance for Industry Orally Disintegrating Tablets, [Online]. Available http://www.fda.gov/cder/guidance/index.htm 2008, Accessed date: 31 October 2018.
[71] A. Gupta, R.L. Hunt, R.B. Shah, V.A. Sayeed, M.A. Khan, Disintegration of highly soluble immediate release tablets: a surrogate for dissolution, AAPS PharmSciTech 10 (2) (Jun. 2009) 495–499.
[72] S. Yassin, et al., The disintegration process in microcrystalline cellulose based tablets, part 1: influence of temperature, porosity and Superdisintegrants, J. Pharm. Sci. 104 (10) (Oct. 2015) 3440–3450.
[73] J.T. Ingram, W. Lowenthal, Mechanism of action of starch as a tablet Disintegrant I, J. Pharm. Sci. 55 (6) (Jun. 1966) 614–617.
[74] A.M. Guyot-Hermann, D.J. Ringard, Disintegration mechanisms of tablets containing starches. Hypothesis about the particle-particle repulsive force, Drug Dev. Ind. Pharm. 7 (2) (Jan. 1981) 155–177.
[75] N.R. Patel, R.E. Hopponent, Mechanism of action of starch as a disintegrating agent in aspirin tablets, J. Pharm. Sci. 55 (10) (Oct. 1966) 1065–1068.
[76] W. Lowenthal, Mechanism of action of starch as a tablet Disintegrant V: effect of starch grain deformation, J. Pharm. Sci. 61 (3) (Mar. 1972) 455–459.
[77] P.M. Hill, Effect of compression force and corn starch on tablet disintegration time, J. Pharm. Sci. 65 (11) (Nov. 1976) 1694–1697.